Cationic Water–Soluble Poly(*p*–Phenylene Vinylene) for Fluorescence Sensors and Electrostatic Self–Assembly Nanocomposites with Quantum Dots

Yang Zhang,[1] Yan Yang,[1] Chang-Chun Wang,[1] Bin Sun,[1] Ying Wang,[1] Xin-Ying Wang,[2] Qun-Dong Shen[1]

[1]*Department of Polymer Science and Engineering and Key Laboratory of Mesoscopic Chemistry (Ministry of Education), School of Chemistry and Chemical Engineering, Nanjing University, Nanjing 210093, China*
[2]*Key Laboratory of Analytical Chemistry for Life Science (Ministry of Education), School of Chemistry and Chemical Engineering, Nanjing University, Nanjing 210093, China*

Received 22 January 2008; accepted 2 June 2008
DOI 10.1002/app.28837
Published online 8 September 2008 in Wiley InterScience (www.interscience.wiley.com).

ABSTRACT: A cationic water-soluble poly(*p*-phenylene vinylene) derivative (poly{2-methoxy-5-[3-(*N*,*N*,*N*-ethyldimethylamino)-1-propoxy]-1,4-phenylene vinylene}bromide) was synthesized by a facile approach. The fluorescence of the conjugated polyelectrolyte was enhanced in the presence of an anionic surfactant because of the regularity of the chain conformation. Meanwhile, its emission was efficiently quenched by a trace amount (10^{-6} mol/L) of the iron complex $Fe(CN)_6^{4-}$ with pronounced quenching efficiency. The cationic conjugated polymer chains were readily assembled on the surface of negatively charged CdTe quantum dots through electrostatic attraction. The resulting nanocomposites facilitated the charge transfer between the conjugated polymers and the quantum dots because of the extensive interfacial area and intimate contact of the two components. © 2008 Wiley Periodicals, Inc. J Appl Polym Sci 110: 3225–3233, 2008

Key words: conjugated polymers; fluorescence; nanocomposites; polyelectrolytes; sensors

INTRODUCTION

Conjugated polymers are a class of "one-dimensional" semiconductors that have electrons delocalized on the π-conjugated backbones. Recently, their unique optical and electronic properties have prompted extensive interest in applications including light-emitting devices, photovoltaic cells, and thin-film transistors.[1–5] Conjugated polymers with anionic or cationic side groups are readily dissolved in aqueous solutions. This opens doors of opportunity for their applications in biosensors. Chen et al.[6,7] first reported that water-soluble conjugated polymers are capable of detecting nanomolar quantities of avidin.[6,7] Subsequently, these polymers were developed to detect various biomolecules, including peptides, proteins, RNAs, and DNAs.[8–17] These applications are mainly based on photoinduced electron transfer or resonance energy transfer between the conjugated polymers and the target molecules. In these cases, electrostatic interaction is of great importance to the occurrence of photoinduced electron transfer or resonance energy transfer during the fluorescence analysis. Significant progress has been achieved in the development of cationic conjugated polymers such as polyfluorene, poly(*p*-phenylene), and polythiophene derivatives for the detection of negatively charged biomolecules.[10–15]

Conjugated polymers have also been recognized as versatile materials in organic photovoltaic cells.[18–20] The devices fabricated from conjugated polymers alone suffer from low solar power conversion efficiencies because of the extremely low electron mobility of the polymers. Thus, high-electron-affinity materials such as semiconductive quantum dots (QDs) have been introduced into conjugated polymers to improve device performance.[21–23] The intimate contact of conjugated polymers and QDs and large interfacial areas are crucial to the charge separation/transfer at the interface and therefore the conversion efficiencies of the composites. Nevertheless, to appropriately manipulate the solubility and fluorescence, the QDs are usually tailored with shells of inorganic materials or organic surfactants. The coating outside is an obstacle to direct contact with the conjugated polymers. Therefore, there is a significant need to design composites with easy charge separation at the interface. Alivisatos et al.[22] directly attached oligothiophene with phosphonic acid groups to CdSe QDs by a ligand-exchange technique.

Correspondence to: Q.-D. Shen (qdshen@nju.edu.cn).
Contract grant sponsor: National Natural Science Foundation of China; contract grant number: 20774040.

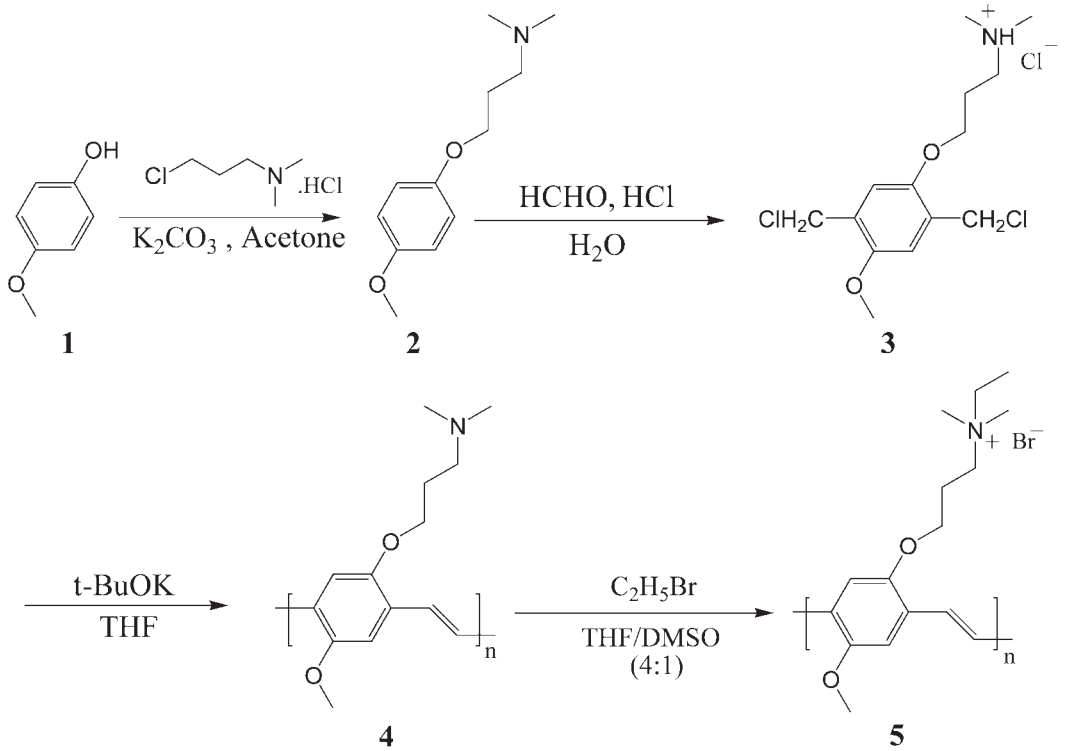

Scheme 1 Brief synthetic route to MPN–PPV.

Emrick et al.[24] grafted poly(*p*-phenylene vinylene) (PPV) to the surface of CdSe QDs. The increased interfacial contact in such composites allows the charge generated in the conjugated polymers to be transferred to the QDs. Meanwhile a good dispersion of the latter in the composite film is achieved. However, the multistep preparation of conjugated polymer/QD composites by the aforementioned methods is relatively complicated and time-consuming and usually has the disadvantages of surface oxidation, size changes, and photoluminescence attenuation of the QDs.

In this study, a cationic water-soluble PPV derivative, poly{2-methoxy-5-[3-(*N,N,N*-ethyldimethylamino)-1-propoxy]-1,4-phenylene vinylene}bromide (MPN–PPV or **5**), was synthesized by a facile approach. The conjugated polyelectrolyte is sensitive to both anionic surfactants and fluorescence quenchers in an aqueous solution, and this indicates its potential applications in chemical and biological sensors. Moreover, a convenient one-step strategy for fabricating conjugated polymer/QD nanocomposites by electrostatic self-assembly is described. The CdTe QDs used here are negatively charged and are widely used in biological applications, and they have been expediently synthesized in a water-phase system.[25–27] We show that positively charged MPN–PPV can be directly assembled outside anionic CdTe QDs through the electrostatic force. The effective surface tailoring of QDs is demonstrated by the fact that the nanocomposite undergoes excited-state charge transfer from MPN–PPV to the QDs.

EXPERIMENTAL

Materials

The cationic PPV derivative was synthesized by a four-step approach (Scheme 1). The CdTe QDs were prepared by established literature procedures and capped with mercaptoacetic acid.[28] Anhydrous tetrahydrofuran (THF) was obtained by distillation over sodium/diphenyl ketone. 3-(Dimethylamino)propyl chloride hydrochloride and potassium *tert*-butoxide from Aldrich (Milwaukee, WI) were used as received. All other chemicals were used without further purification.

Characterization

^{1}H-NMR spectra were collected on a Bruker DPX300 spectrometer (Bruker, Switzerland). Ultraviolet–visible (UV–vis) and fluorescence spectra were measured on a Shimadzu UV-3100 spectrophotometer and AB2 luminescence spectrometer, respectively. The morphology via atomic force microscopy (AFM) was obtained with a NanoScope IIIa (Digital Instruments).

Synthesis

3-(4-Methoxyphenoxy)-*N,N*-dimethylpropan-1-amine (**2**)

Potassium carbonate (22.2 g), 4.86 g of 4-methoxy phenol (**1**), and 150 mL of acetone were mixed and stirred in advance, and then 4.76 g of 3-(dimethylamino)propyl chloride hydrochloride was added to the mixture under a nitrogen atmosphere. After intense stirring for 72 h with refluxing, the precipitate was filtered, and the acetone was evaporated at reduced pressure. Ethyl acetate (100 mL) was added to the residue and washed with water three times and with brine once, and then it was dried over anhydrous magnesium sulfate. After the solvent was evaporated, the residue was added to excessive 1 mol/L hydrochloric acid and stirred for 1 h at room temperature. This solution was washed with ethyl acetate three times, and then 1 mol/L potassium carbonate was added dropwise into the solution until all the organic oily product was precipitated from the water layer. The organic layer was extracted with ethyl acetate, and the extract was washed with water three times and with brine once and then was dried over anhydrous magnesium sulfate. After the solvent was removed, 5.14 g of yellow liquid was obtained (yield = 82%).

^{1}H-NMR ($CDCl_3$, δ, ppm): 1.97 (2H, —CCH_2C—, m), 2.27 (6H, —NCH_3, s), 2.48 (2H, —CCH_2N—, t), 3.70 (3H, —O—CH_3, s), 3.98 (2H, —OCH_2C—, t), 6.83 (4H, —C_6H_4—, s).

5-Methoxy-2-[3-(*N,N*-dimethylamino)-1-propoxy]-1, 4-xylene-α,α′-dichloride hydrochloride (**3**)

A 37% formalin solution (11.25 mL), 16.80 mL of water, 11.25 mL of concentrated hydrochloric acid, and 3.0 g of compound **2** were mixed in a three-necked bottle, and the mixture was cooled to 2°C. A stream of hydrogen chloride gas was bubbled through the mixture for 45 min, and then the temperature was increased to 45°C. The mixture was saturated with hydrogen chloride throughout the period, and the reaction was stopped 30 min later. Then, nitrogen gas was bubbled into the mixture until a white precipitate was observed. The precipitate was centrifuged and washed with acetone. After a period of drying *in vacuo*, 2.06 g of a gray-white product was collected (yield = 42%).

^{1}H-NMR [dimethyl sulfoxide-d_6 (DMSO-d_6), δ, ppm]: 2.12 (2H, —CCH_2C—, m), 2.76 (6H, —NCH_3, s), 3.23 (2H, —CCH_2N—, t), 3.70 (3H, —O—CH_3, s), 4.07 (2H, —OCH_2C—, t), 4.74 (4H, —OCH_2Cl, s), 7.17 (2H, —C_6H_2—, s).

Poly{2-methoxy-5-[3-(*N,N*-dimethylamino)-1-propoxy]-1,4-phenylene vinylene} (**4**)

Under a dry nitrogen atmosphere, 0.7 g of compound **3** was mixed with 50 mL of anhydrous THF in a 100-mL, round-bottom flask. To this stirred solution was added dropwise 16.47 mL of a 20% solution of potassium *tert*-butoxide in anhydrous THF. The mixture was stirred at the ambient temperature for 24 h. Then, the reaction mixture was poured into methanol with stirring. The resulting red precipitate was washed with water and dried *in vacuo* to obtain 0.2 g of a red powder (yield = 42%).

^{1}H-NMR ($CDCl_3$, δ, ppm): 2.1 (2H, —CCH_2C—), 2.3 (6H, —NCH_3), 2.6 (2H, —CCH_2N—), 3.9–4.2 (5H, —OCH_2C—, —O—CH_3, m), 7.1–7.4 (4H, —CH=CH—, —C_6H_2—, m).

Poly{2-methoxy-5-[3-(*N,N,N*-ethyldimethylamino)-1-propoxy]-1,4-phenylene vinylene}bromide (**5**)

A 50-mL, round-bottom flask with a magnetic stirring bar was charged with 0.1 g of polymer **4**. The polymer was dissolved in 20 mL of THF and 5 mL of DMSO. Then, 0.5 g of bromoethane was added, and the solution was stirred at 50°C for 3 days. The polymer was precipitated in 100 mL of acetone and collected by centrifugation. The precipitates were redissolved in distilled water and dialyzed with a membrane with a 8000–10,000 cutoff for 3 days. After a period of drying *in vacuo*, 0.1 g of the product was obtained (yield = 68%).

^{1}H-NMR (1/2 v/v D_2O/DMSO-d_6, δ, ppm): 1.2 (—NCH_2CH_3), 2.2–2.4 (—CCH_2C—, m), 3.0 (—NCH_3), 3.2–3.4 (—NCH_2CH_3, —CCH_2N—, m), 3.8–4.0 (—OCH_2C—, —O—CH_3, m), 6.8–7.5 (—CH=CH—, —C_6H_2—, m).

RESULTS AND DISCUSSION

Basic photophysics of MPN–PPV in solution

The UV–vis absorption and fluorescence emission spectra of a diluted MPN–PPV aqueous solution (20 μmol/L) are shown in Figure 1. The cationic conjugated polymer has an optical absorption peak at 416 nm, which arises from π-electron transitions from delocalized occupied molecular orbitals to delocalized unoccupied ones. The edge absorption of MPN–PPV in the aqueous solution is at 520 nm, corresponding to an optical band gap of 2.38 eV. Once MPN–PPV in water is photoexcited, it returns to the ground state by the emission of green light with a maximum wavelength of 530 nm.

The choice of solvents has significant effects on the fluorescence intensity of the conjugated polymer. With the addition of methanol to an aqueous solution, the emission of MPN–PPV is dramatically enhanced (Fig. 2). The fluorescence of the polymer in the methanol solution is almost 7 times as strong as that in an aqueous solution. In Figure 1, the emission spectra in methanol and water have been

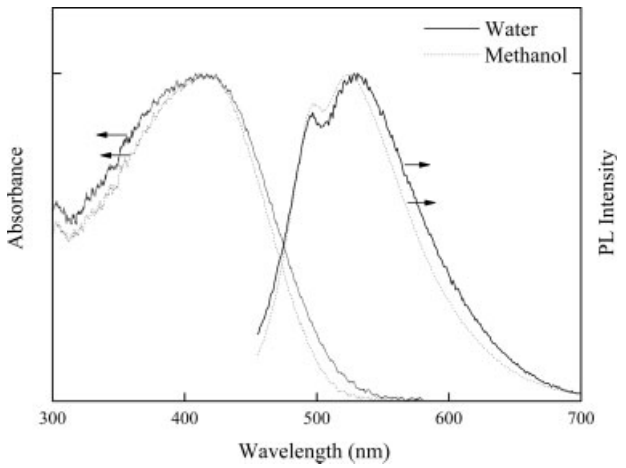

Figure 1 Electron absorption and photoluminescence spectra (excitation wavelength = 450 nm) of MPN–PPV in an aqueous solution and in methanol.

normalized to the same maximum values for better comparison, and both show two discernible peaks. Slight blueshifts (<5 nm) of the emission maxima, as well as absorption peaks, can be observed when the water is replaced by methanol.

MPN–PPV has positively charged ammonium side groups that produce its solubility in water. Their chains in a diluted aqueous solution are presumably isolated. Nevertheless, the nonpolar phenylene vinylene backbone of MPN–PPV is incompatible with water. Such amphiphilic polymer chains in an aqueous medium tend to pack together in an aggregated, π-stacked configuration and adopt a structure in which the hydrophobic units are tucked inside and the hydrophilic units are exposed to water. The evidence of hydrophobic interactions comes from ^{1}H-NMR spectra of the MPN–PPV solution (Fig. 3). In the D_2O solution, the aromatic and vinylene protons of the polymer backbone show broad peaks in the region of 6–8 ppm, which are totally overlapped and difficult to distinguish. The poor resolution of the NMR spectrum in the D_2O solution is the result of aggregation of aromatic rings. This part of the polymer chain is insoluble in deuterium oxide. In the D_2O/DMSO-d_6 (1/2 v/v) solution, resonance signals become sharp, and this means that DMSO is a good solvent for the conjugated backbone, so dissociation of the aggregates takes place.

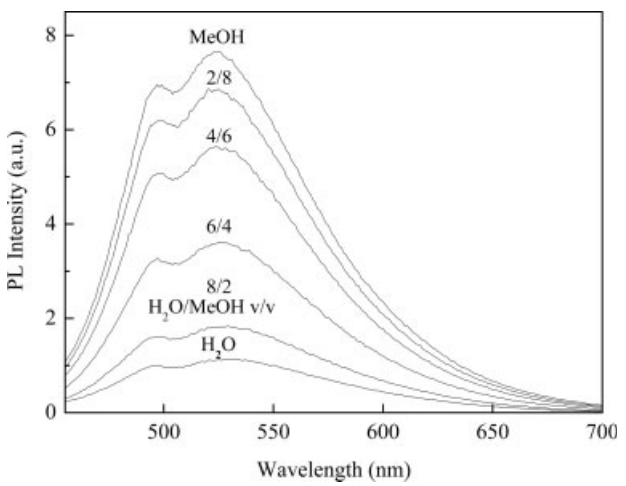

Figure 2 Influence of the methanol content on the fluorescence spectra (excitation wavelength = 450 nm) of MPN–PPV (20 μmol/L).

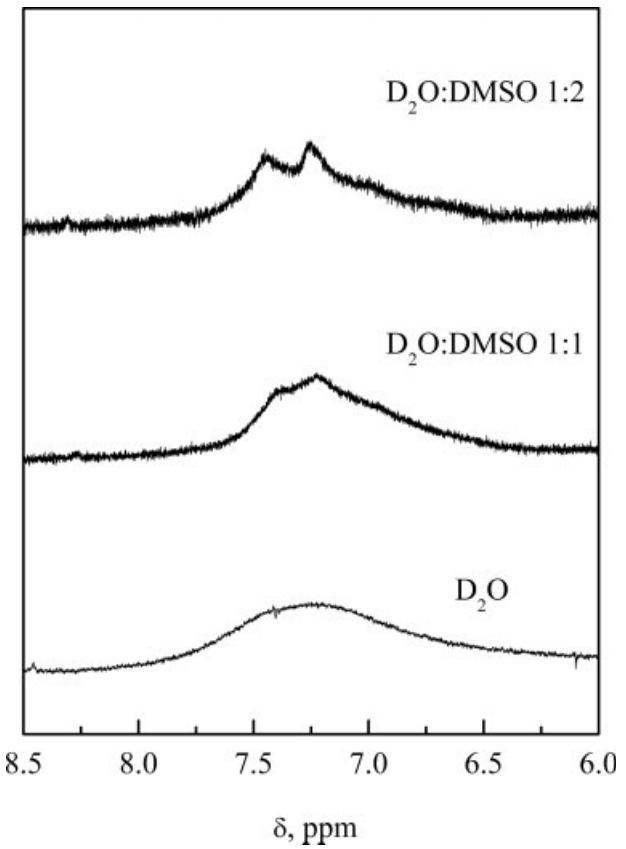

Figure 3 ^{1}H-NMR spectra of MPN–PPV in deuterium oxide and a mixed solvent (D_2O/DMSO-d_6).

The photoluminescence of a single conjugated chain mainly comes from intrachain excitons. In contrast, the aggregated states of two or more polymer chain segments are weakly emissive because of the delocalization of electronic wave function over multiple chromophores. The formation of interchain or intrachain aggregations is often signaled by the decrease in the quantum yield and the redshift of the emission.[29,30] The solvent effect originates from the formation or dissociation of the aggregations. Organic solvents such as methanol have a preferential interaction with the hydrophobic aromatic backbone of MPN–PPV. When methanol gradually takes the place of water, weakly emissive interchain species are partially replaced by highly emissive intrachain excitons. This results in notable recovery of the fluorescence and a slight blueshift of the emission peaks.

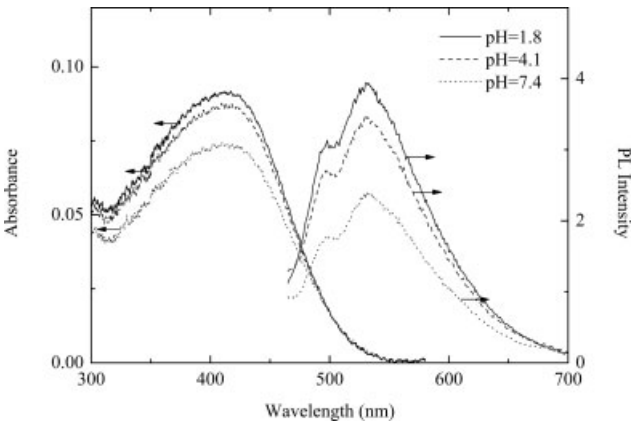

Figure 4 Electron absorption and fluorescence spectra of MPN–PPV in an aqueous solution (20 μmol/L) as a function of the pH.

To evaluate the effect of other environmental factors, the fluorescence spectra of MPN–PPV in aqueous solutions at pH values ranging from 1.8 to 7.4 have been investigated (Fig. 4). The emission intensity of MPN–PPV is dramatically enhanced with a lowering of the pH value, and this indicates improved solubility of the polymer in an acidic aqueous solution. The postpolymerization quaternization approach is adopted to realize water solubility of the precursor polymer (**4**) with amino-functional groups. After treatment with bromoethane, a quaternization degree of about 50% can be estimated from the relative integrals corresponding to the $-NCH_2-$ and $-NCH_3$ resonances in the ^{1}H-NMR spectra. MPN–PPV dissolves very well in an acid solution by protonation of the remaining amino groups. The improvement in the fluorescence efficiency is consistent with the dissociation of weakly emissive aggregates in water.

With the increase in the emission intensity in the acid solution, there are no discernable shifts of the optical absorption or emission maxima of the polymer. It is evident that the proton-induced conformational change of the MPN–PPV chains, if there is any, is too weak to be observed.

Fluorescence enhancement by the cationic surfactant

Electrostatic interactions of water-soluble conjugated polymers with oppositely charged fluorescence quenchers, peptides, proteins, RNAs, DNAs, and surfactants are of critical importance to their sensory signal transduction. On the other hand, polyelectrolyte complexes with guest molecules such as fluorescent dyes, surfactants, and proteins have attracted substantial attention. This is driven by fundamental interest in their supramolecular structure and numerous current or foreseen applications. Small-molecule fluorescence probe techniques have also been developed as powerful tools for investigating polymer–surfactant systems. Nevertheless, less attention has been paid to the photophysical properties of fluorescent conjugated polyelectrolyte complexes with surfactants.[8,31]

When the anionic surfactant [sodium dodecyl sulfate (SDS)] is added to a diluted MPN–PPV solution in a stepwise manner, a noticeable increase of the fluorescence intensity can be detected (Fig. 5). The emission can be 3.4 times as strong as the original intensity in the presence of 20 μmol/L SDS. Meanwhile, a progressive redshift of the emission peak can be observed with the involvement of SDS. It is well established that the emission maxima may be redshifted by an increase in the chain conjugation length or aggregation degree. In the latter case, the emission intensity is expected to drop because of an increase in the nonradiative relaxation, and this disagrees with the current results. Therefore, the MPN–PPV/SDS complexes should have a longer average conjugation length than the conjugated polymer alone. A redshift of the absorption spectrum of MPN–PPV in the presence of SDS (the inset of Fig. 5) can also be observed, as expected.

The dependence of fluorescence spectra on the excitation wavelength gives more insight into the structural change of MPN–PPV chains during complexation. As shown in Figure 6(a), the emission spectra of MPN–PPV alone are strongly dependent on the excitation wavelength. The maximum emission wavelength is located at 492 nm with excitation at 420 nm, whereas the emission maximum redshifts to 530 nm, arising when the polymer is excited at 450 nm. With the addition of SDS, the emission

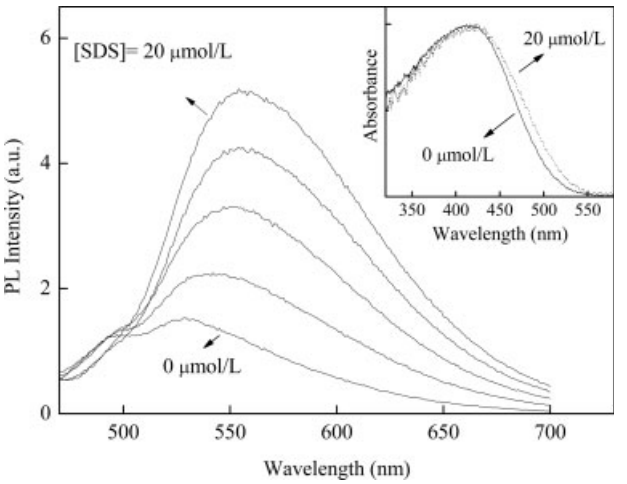

Figure 5 Emission behaviors of a diluted aqueous solution of MPN–PPV (20 μmol/L) in the presence of an anionic surfactant ([SDS] = 0–20 μmol/L at intervals of 5 μmol/L; excitation wavelength = 450 nm). The inset shows normalized UV–vis spectra of MPN–PPV with and without SDS.

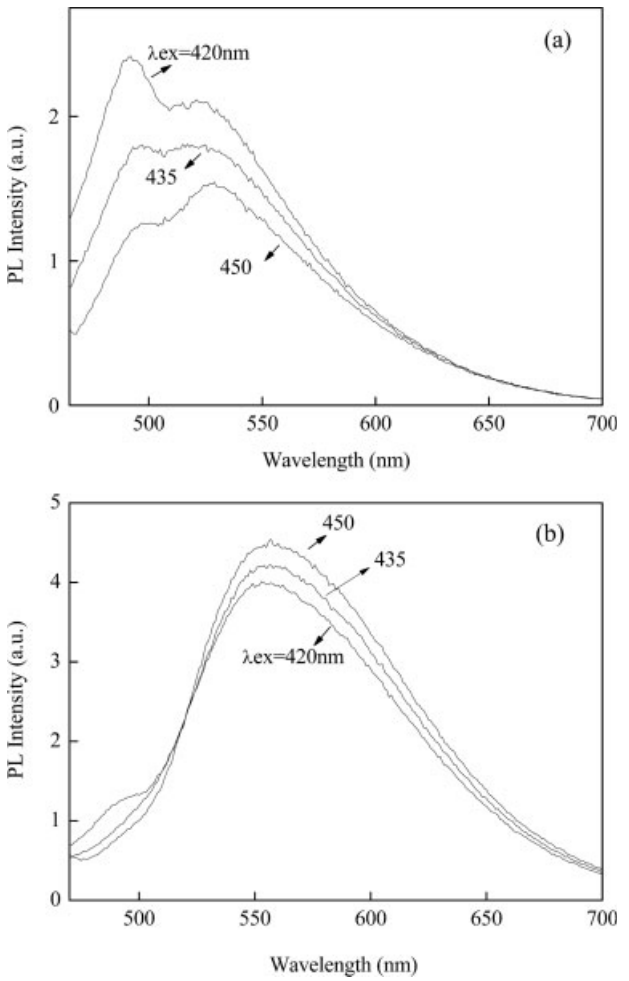

Figure 6 Dependence of the emission spectra of MPN–PPV (20 μmol/L) on the excitation wavelengths: (a) MPN–PPV alone in water and (b) MPN–PPV in the presence of SDS (15 μmol/L).

spectra of MPN–PPV become excitation-wavelength-independent [Fig. 6(b)]. Such behavior indicates a broad distribution of the conjugation lengths in aqueous solutions, which arises from the chain conformational disorder.

When SDS molecules are introduced into a solution, the individual MPN–PPV chains attract negatively charged head groups of the surfactants. The complexation takes place at SDS concentrations considerably lower than its critical micelle concentration (ca. 8 mmol/L).[32] The conjugated polymer chains are surrounded by hydrophobic surfactant tails. As a result, an extended chain conformation of the polymer will favor orderly packing of the surfactants and reduce the exposure of the hydrophobic tails to water. Previous studies have shown that most polyelectrolyte chains take more extended conformations during their complexation with surfactants. Their complexes can be regarded as comb-shaped polymers with surfactants as side chains, and the surfactants tend to self-assemble into layered structures.[33] The resulting regular chain conformations contribute to the excitation-independent emission spectra of MPN–PPV. The formation of complexes between MPN–PPV and SDS also reduces the number of kink defects on the chains and suppresses the aggregation of the hydrophobic backbones. Thus, the fluorescence quantum efficiency of MPN–PPV is markedly increased by the addition of an anionic surfactant.

The two peaks existing in the fluorescence spectra might arise from the presence of two chromophores or a bimodal distribution of conjugation lengths due to different chain lengths or chemical defects on the conjugated backbones. However, the distribution of conjugation lengths caused by chain conformation disorder is the most likely reason because the addition of the surfactant mainly changes the conformation of polymer chains and cannot eliminate the chemical defects or reduce the number of the chromophores. According to Figure 6, the addition of SDS reduces the proportion of higher energy peaks with an obvious intensity increase of the lower energy peak. Thus, the chain conformation disorder may be responsible for the two peaks in the spectra.

The addition of surfactants may change the ionic strength of a solution. To take the ionic effect into consideration, we further studied the fluorescence of MPN–PPV in phosphate-buffered saline buffer solutions (pH = 7.4) with different salt concentrations. As shown in Figure 7, the influence of a low concentration (10^{-4} mol/L) of NaCl on the polymer emission is inconspicuous. However, when the salt concentration increases by 2 or 3 orders of magnitude, the salt effect becomes obvious. The photoluminescence intensity of MPN–PPV is reduced to 60% with 0.1 mol/L NaCl in the buffer. The phenomenon is the opposite of that of the SDS system. By the addition of NaCl, the electrostatic repulsion

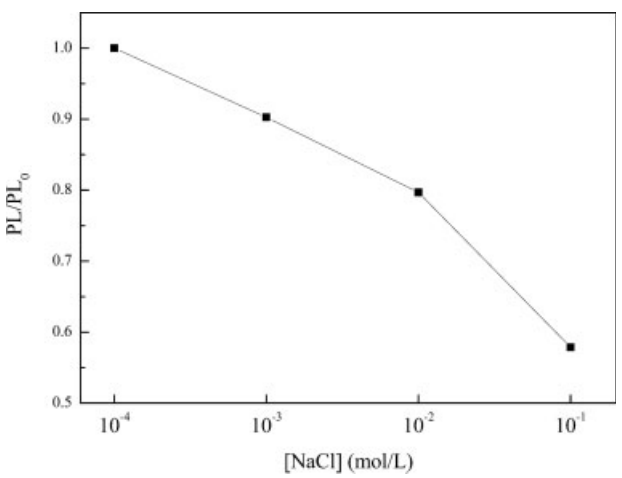

Figure 7 Emission behavior of a diluted aqueous solution of MPN–PPV (20 μmol/L, pH = 7.4) in the presence of sodium chloride (excitation wavelength = 450 nm).

between positive ammonium groups is effectively screened. The weakened electrostatic repulsion may lead to the folding of the polymer chains (or the conformational disorder) and interchain aggregation driven by hydrophobic interactions, that is, π-stacking of aromatic rings. Both have been proved to be adverse to exciton radiative relaxation.

Fluorescence response in the presence of a small-molecule quencher

The photoluminescence of MPN–PPV in a diluted aqueous solution is highly sensitive to the presence of the quencher molecules of $Fe(CN)_6^{4-}$. As shown in Figure 8, the quencher concentration required to lose half of the original fluorescence intensity is about 3×10^{-6} mol/L. The fluorescence of MPN–PPV can be almost completely quenched by a rather low quencher concentration ($<10^{-5}$ mol/L). The quenching mechanism is mainly due to static or dynamic charge transfer from excited species in conjugated polymers to $Fe(CN)_6^{4-}$.

According to the Stern–Volmer equation, the evolution of fluorescence as a function of the quencher concentration ([Q]) can be expressed as follows:

$$\frac{PL_0}{PL} = 1 + K_{SV}[Q] \quad (1)$$

where PL_0 and PL are the steady-state fluorescence intensities in the absence and presence of the quencher, respectively. K_{SV} is the Stern–Volmer constant, which provides a direct measurement of the quenching efficiency or sensitivity. A linear Stern–Volmer relationship can be found when $[Fe(CN)_6^{4-}]$ is less than 5×10^{-6} mol/L (inset of Fig. 8), and K_{SV} is 3.2×10^5 $(mol/L)^{-1}$. The latter is about 2×10^4 times larger than that of a small-molecule fluorescence quenching system such as stilbene and methylviologen.[6] The pronounced quenching efficiency arises from the "molecular wire" effect described by Swager and Zhou.[34,35] Binding of the quencher to MPN–PPV and extremely rapid diffusion of photoinduced excitons along the polymer main chain to the trapped quencher increase the probability of charge transfer and aggressively amplify fluorescence quenching.

As shown in the inset of Figure 8, after deconvolution of the two peaks with respect to the bimodal distribution of the conjugated lengths, it is found that the lower energy peak is more sensitive to quenching. When only the lower energy peak is considered, the plot is also nonlinear. As far as we know, nonlinear quenching is prevalent in conjugated polymer–quencher systems.[12,36] As for ref. 36, with respect to the higher energy peak, the lower energy peak (long conjugated chains) exhibits obviously amplified quenching due to the high delocalization of singlet excitons and the rapidness of the energy migration along the conjugated backbone. The upward Stern–Volmer curve observed for the fluorescence quenching of long conjugated chains can be explained by the existence of a sphere of action for polymer chains in aqueous solutions,[37] which can be described by the modified Stern–Volmer equation:

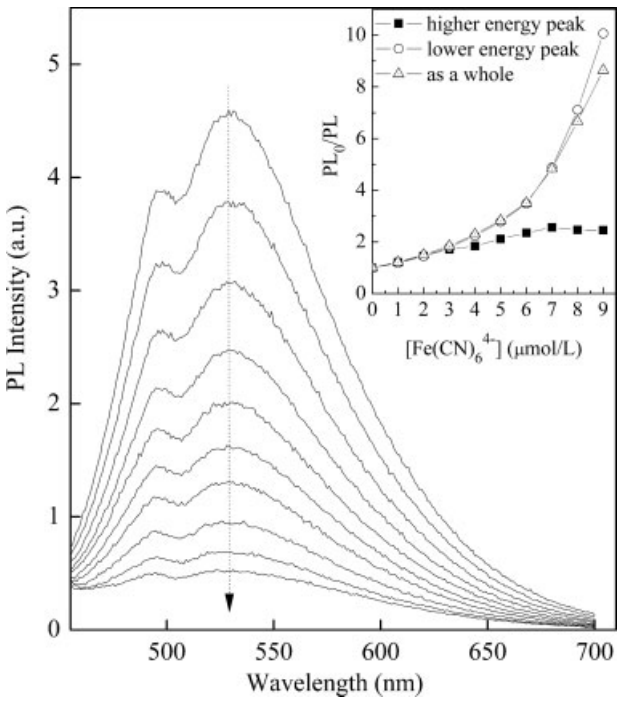

Figure 8 Response of the fluorescence of MPN–PPV (50 μmol/L) to the anionic quencher ($[Fe(CN)_6^{4-}]$ = 0–9 μmol/L at intervals of 1 μmol/L; excitation wavelength = 450 nm). The inset shows Stern–Volmer quenching plots.

$$\frac{PL_0}{PL} = (1 + K_{SV}[Q])e^{\alpha V[Q]} \quad (2)$$

where V is the volume constant and α is used to account for the charge-induced enhancement of the local quencher concentration.

Conjugated polymer/QD nanocomposites

QDs and conjugated polymers are complementary in their electronic properties. The former have a high electron affinity, and the latter are hole-accepting. Their nanocomposites have been exploited as hybrid inorganic/organic electroluminescent devices and solar cells. Here we present a facile electrostatic assembly strategy for fabricating core/shell nanocomposites of a water-soluble conjugated polymer and CdTe QDs capped with mercaptoacetic acid. Figure 9(a) shows the response of the CdTe QD fluorescence to the addition of MPN–PPV. The maximum emission wavelength of the QDs is located at 570

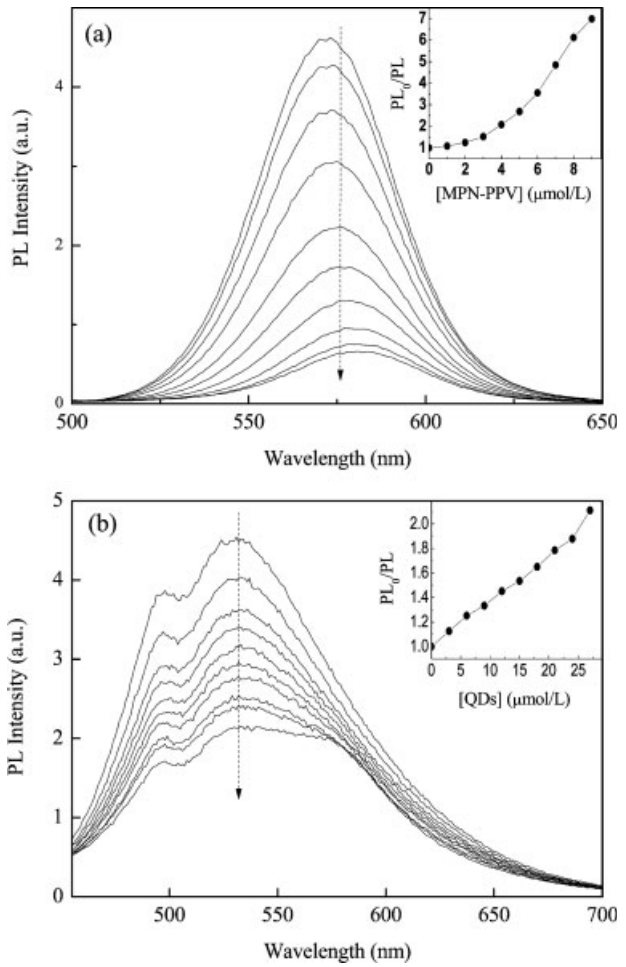

Figure 9 (a) Emission behavior of CdTe QDs (30 μmol/L) in the presence of MPN–PPV (from 0 to 9 μmol/L at intervals of 1 μmol/L). The inset shows Stern–Volmer quenching plots. (b) Change in the fluorescence intensity of MPN–PPV (50 μmol/L) upon the addition of CdTe QDs (from 0 to 27 μmol/L at intervals of 3 μmol/L; excitation wavelength = 450 nm). The inset shows Stern–Volmer quenching plots.

nm, and the room-temperature fluorescence quantum efficiency is 28%. Remarkable photoluminescence attenuation can be observed where the CdTe QD emission can be drastically quenched to about 14% of its original intensity in the presence of a trace amount (9 μmol/L) of MPN–PPV. At the same time, the CdTe QDs weaken the conjugated polymer luminescence as well [Fig. 9(b)]. The Stern–Volmer plot demonstrates hyperefficient quenching with a K_{SV} value of about 3.8×10^4 $(mol/L)^{-1}$.

The fluorescence quenching of both the conjugated polymer and the QDs are well described by charge transfer between them, by which photoexcited species would subsequently return to the ground state in a nonradiative manner. Efficient charge transfer requires both matched electronic energy levels and intimate contact between electron donors and acceptors. The mercaptoacetic acid capped QDs are negatively charged in an aqueous solution. Thus, the positively charged MPN–PPV chains can assemble on their surface by electrostatic adhesion. The formation of nanocomposites allows the conjugated polymer and the QDs in close proximity to make charge transfer possible. It is well established that there exists rapid charge separation at the interface of poly[2-methoxy-5-(2′-ethyl) hexyloxy-*p*-phenylene vinylene] (MEH–PPV)/CdSe QD composites.[23] MEH–PPV and MPN–PPV share the same conjugated backbone and similar energy levels. Therefore, the electron transfer between MPN–PPV and QDs is energetically favorable as well.

In conjugated polymer/QD nanocomposites, a uniform dispersion of the inorganic nanoparticles is beneficial to the improvement of optoelectronic device performance. Such a dispersion is difficult to obtain because the nanoparticles tend to aggregate in the polymer matrix. In our case, anionic QDs are coated by a cationic conjugated polymer in the solution. It is expected that the nanoparticles will disperse well in the resulting composite film. Figure 10 shows the AFM image of a MPN–PPV/CdTe QD (40 wt %) nanocomposite film cast on indium tin oxide glass. The topographic image of the solid film exhibits a relatively smooth surface morphology with a root mean square value of 0.632 nm. There is no obvious phase separation in the nanocomposite film. The intimate connection of the polymer to the QD surface and extensive interfacial area would profoundly impact the photophysics of the resulting nanocomposites.

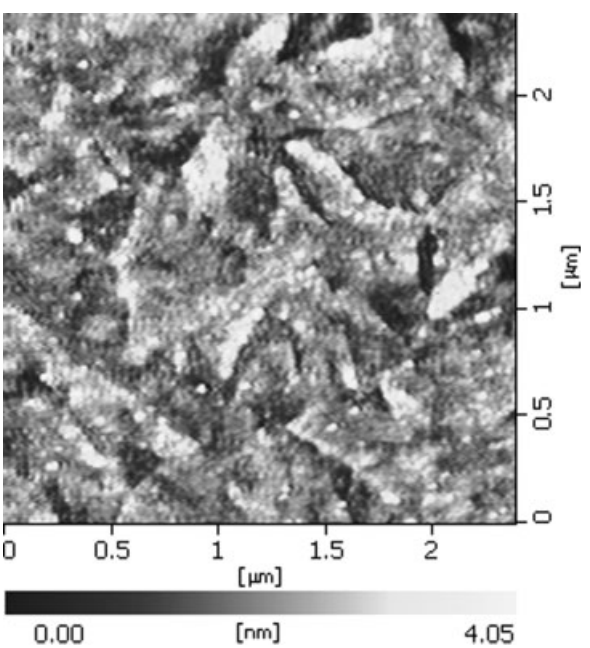

Figure 10 AFM image of the MPN–PPV/CdTe QD (40 wt %) nanocomposite film on indium tin oxide glass.

CONCLUSIONS

We have investigated a novel cationic water-soluble PPV derivative (MPN–PPV) with potential applications in fluorescence sensors and optoelectronic devices. The emission intensity of MPN–PPV responds sensitively to the existence of surfactants and iron complex quenchers. Furthermore, the conjugated polyelectrolytes can assemble on the surface of QDs through electrostatic attraction and favor efficient charge transfer between them. The resulting uniform dispersion of the QDs in the conjugated polymer matrix together with the intimate contact of the two components makes the nanocomposites promising materials for the fabrication of high-efficiency photovoltaic cells.

The authors thank Jun-Sheng Yu at the Key Laboratory of Analytical Chemistry for Life Science (Ministry of Education) of Nanjing University.

References

1. Burroughes, J. H.; Bradley, D. D. C.; Brown, A. R.; Marks, R. N.; Mackay, K.; Friend, R. H.; Burns, P. L.; Holmes, A. B. Nature 1990, 347, 539.
2. Granstrom, M.; Petritsch, K.; Arias, A. C.; Lux, A.; Andersson, M. R.; Friend, R. H. Nature 1998, 395, 257.
3. Brabec, C. J.; Sariciftci, N. S.; Hummelen, J. C. Adv Funct Mater 2001, 11, 15.
4. Sirringhaus, H.; Tessler, N.; Friend, R. H. Science 1998, 280, 1741.
5. Huitema, H. E. A.; Gelinck, G. H.; van der Putten, J. B. P. H.; Kuijk, K. E.; Hart, C. M.; Cantatore, E.; Herwig, P. T.; van Breemen, A. J. J. M.; de Leeuw, D. M. Nature 2001, 414, 599.
6. Chen, L.; McBranch, D. W.; Wang, H. L.; Helgeson, R.; Wudl, F.; Whitten, D. G. Proc Natl Acad Sci U S A 1999, 96, 12287.
7. Heeger, P. S.; Heeger, A. J. Proc Natl Acad Sci U S A 1999, 96, 12219.
8. Chen, L.; Xu, S.; McBranch, D.; Whitten, D. J Am Chem Soc 2000, 122, 9302.
9. Gaylord, B. S.; Wang, S.; Heeger, A. J.; Bazan, G. C. J Am Chem Soc 2001, 123, 6417.
10. Ho, H. A.; Boissinot, M.; Bergeron, M. G.; Corbeil, G.; Doré, K.; Boudreau, D.; Leclerc, M. Angew Chem Int Ed 2002, 41, 1548.
11. Wang, S.; Bazan, G. C. Adv Mater 2003, 15, 1425.
12. Fan, C.; Wang, S.; Hong, J. W.; Bazan, G. C.; Plaxco, K. W.; Heeger, A. J. Proc Natl Acad Sci U S A 2003, 100, 6297.
13. Feng, F. D.; Tang, Y. L.; He, F.; Yu, M. H.; Duan, X. R.; Wang, S.; Li, Y. L.; Zhu, D. B. Adv Mater 2007, 19, 3490.
14. Liu, B.; Bazan, G. C. Proc Natl Acad Sci U S A 2005, 102, 589.
15. Peng, H.; Soeller, C.; Travas-Sejdic, J. Chem Commun 2006, 3735.
16. You, C. C.; Miranda, O. R.; Gider, B.; Ghosh, P. S.; Kim, I. B.; Erdogan, B.; Krovi, S. A.; Bunz, U. H. F.; Rotello, V. M. Nat Nanotechnol 2007, 2, 318.
17. Chi, C. Y.; Mikhailovsky, A.; Bazan, G. C. J Am Chem Soc 2007, 129, 11134.
18. Halls, J. J. M.; Walsh, C. A.; Greenham, N. C.; Marseglia, E. A.; Friend, R. H.; Moratti, S. C.; Holmes, A. B. Nature 2005, 376, 498.
19. Yu, G.; Gao, J.; Hummelen, J. C.; Wudl, F.; Heeger, A. J. Science 1995, 270, 1789.
20. Sariciftci, N. S.; Smilowitz, L.; Heeger, A. J.; Wudl, F. Science 1992, 258, 1474.
21. Huynh, W. U.; Dittmer, J. J.; Alivisatos, A. P. Science 2002, 295, 2425.
22. Milliron, D. J.; Alivisatos, A. P.; Pitois, C.; Edder, C.; Fréchet, J. M. J. Adv Mater 2003, 15, 58.
23. Greenham, N. C.; Peng, X.; Alivisatos, A. P. Phys Rev B 1996, 54, 17628.
24. Skaff, H.; Sill, K.; Emrick, T. J Am Chem Soc 2004, 126, 11322.
25. Gao, M. Y.; Kirstein, S.; Möhwald, H.; Rogach, A. L.; Kornowski, A.; Eychmüller, A.; Weller, H. J Phys Chem B 1998, 102, 8360.
26. Gaponik, N.; Talapin, D. V.; Rogach, A. L.; Hoppe, K.; Shevchenko, E. V.; Kornowski, A.; Eychmüller, A.; Weller, H. J Phys Chem B 2002, 106, 7177.
27. Zhang, H.; Zhou, Z.; Yang, B.; Gao, M. Y. J Phys Chem B 2003, 107, 8.
28. Deng, D. W.; Qin, Y. B.; Yang, X.; Yu, J. S.; Pan, Y. J Cryst Growth 2006, 296, 141.
29. Nguyen, T.-Q.; Martini, I. B.; Liu, J.; Schwartz, B. J. J Phys Chem B 2000, 104, 237.
30. Nguyen, T.; Schwartz, B. J. J Chem Phys 2002, 116, 8198.
31. Gu, Z.; Bao, Y.-J.; Zhang, Y.; Wang, M.; Shen, Q.-D. Macromolecules 2006, 39, 3125.
32. Loh, W.; Teixeira, L. A. C.; Lee, L.-T. J Phys Chem B 2004, 108, 3196.
33. Macknight, W. J.; Ponomarenko, E. A.; Tirrell, D. A. Acc Chem Res 1998, 31, 781.
34. Swager, T. M. Acc Chem Res 1998, 31, 201.
35. Zhou, Q.; Swager, T. M. J Am Chem Soc 1995, 117, 7017.
36. Fan, Q. L.; Zhou, Y.; Lu, X. M.; Hou, X. Y.; Huang, W. Macromolecules 2005, 38, 2927.
37. Wang, J.; Wang, D. L.; Miller, E. K.; Moses, D.; Bazan, G. C.; Heeger, A. J. Macromolecules 2000, 33, 5153.